HHS Public Access

Author manuscript

Comp Biochem Physiol C Toxicol Pharmacol. Author manuscript; available in PMC 2019 June 01.

Published in final edited form as:

Comp Biochem Physiol C Toxicol Pharmacol. 2018 June ; 208: 87–95. doi:10.1016/j.cbpc.2017.09.009.

Fluorescent Light Exposure Incites Acute and Prolonged Immune Responses in Zebrafish (*Danio rerio*) Skin

Trevor J. Gonzalez, **Yuan Lu**, **Mikki Boswell**, **William Boswell**, **Geraldo Medrano**, **Sean Walter**, **Samuel Ellis**, **Markita Savage**, **Zoltan M. Varga**[2], **Christian Lawrence**[3], **George Sanders**[4], and **Ronald B. Walter**[*]

Xiphophorus Genetic Stock Center, Department of Chemistry and Biochemistry, 419 Centennial Hall, Texas State University, 601 University Drive, San Marcos, TX 78666 USA

[2]Zebrafish International Resource Center (ZIRC), 5274 University of Oregon Eugene, OR 97403 USA

[3]Children's Hospital Boston Karp Family Research Laboratories, 4th Floor One Blackfan Circle Boston, MA 02115 USA

[4]Department of Comparative Medicine, School of Medicine, University of Washington, Seattle, WA 98195-7340

Abstract

Artificial light produces an emission spectrum that is considerably different than the solar spectrum. Artificial light has been shown to affect various behavior and physiological processes in vertebrates. However, there exists a paucity of data regarding the molecular genetic effects of artificial light exposure. Previous studies showed that one of the commonly used fluorescent light source (FL; 4,100 K or “cool white”) can affect signaling pathways related to maintenance of circadian rhythm, cell cycle progression, chromosome segregation, and DNA repair/recombination in the skin of male *Xiphophorus maculatus*. These observations raise questions concerning the kinetics of the FL induced gene expression response, and which biological functions become modulated at various times after light exposure. To address these questions, we exposed zebrafish to 4,100 K FL and utilized RNA-Seq to assess gene expression changes in skin at various times (1 to 12 hrs) after FL exposure. We found 4,100 K FL incites a robust early (1–2 hrs) transcriptional response, followed by a more protracted late response (i.e., 4–12 hrs). The early transcriptional response involves genes associated with cell migration/infiltration and cell proliferation as part of an overall increase in immune function and inflammation. The protracted late transcriptional response occurs within gene sets predicted to maintain and perpetuate the inflammatory response, as well as suppression of lipid, xenobiotic, and melatonin metabolism.

[*]Corresponding author: Ronald B. Walter, Phone: 512-245-0357, Fax: 512-245-1922, RWalter@txstate.edu, The *Xiphophorus* Genetic Stock Center, Department of Chemistry and Biochemistry, Texas State University, Centennial Hall 419, 601 University Drive, San Marcos, TX 78666, USA.

Keywords

Fluorescent light; zebrafish; vertebrate; skin; RNA-Seq

Introduction

Light is one of the most significant environmental factors that regulate physiological processes. All fluorescent light (FL) sources have different energy distributions across the visible spectrum, particularly when compared to natural sunlight (Fig. 1a; McColl and Veitch, 2001). FL is ubiquitous in areas of human activity (e.g., households, offices, factories and research facilities). Over the last half century the duration of FL exposure by humans and other animals has substantially increased. Despite increased presence and prolonged exposure to FL, potential adverse health effects due to FL exposure have only recently begun to be elucidated. In humans, FL has been shown to affect several physiological processes such as oxygen intake, heart rate and absorption of vitamins and minerals (Holick, 1996; McColl and Veitch, 2001; Wurtman, 1975a, b). FL is also reported to disrupt normal circadian cycles, and has been associated with increased incidence of select diseases (Blask, 2009; Blask et al., 2005; Cajochen et al., 2005; Koo et al., 2016; Lewy et al., 1980; Lucassen et al., 2016; Ohayon and Milesi, 2016; Romeo et al., 2017; Schwimmer et al., 2014; Stevens et al., 2013). Different wavelengths of light have also been shown to suppress melatonin secretion (Brainard et al., 1985; Thapan et al., 2001). However, except for our recent reports, specific responses in gene expression that occur when an intact animal is exposed to various types of FL have not been extensively studied (Boswell et al., 2015; Chang et al., 2015; Contreras et al., 2014; Lu et al., 2015; Walter et al., 2014; Walter et al., 2015; Yang et al., 2014).

We hypothesize that skin is a primary light-receiving organ in fish due to direct interaction with the external environment. Opsins are primary photo-receiving proteins with the ability to transduce a light stimulus into a cellular response. While opsin gene expression is typically associated with the eye, almost all opsins are also expressed in human skin (Haltaufderhyde et al., 2015; Kojima et al., 2011; Leung and Montell, 2017; Tsutsumi et al., 2009). It has been shown that knockdown of rhodopsin in primary human epidermal melanocytes and keratinocytes results in reduced Ca^{2+} flux in response to ultraviolet A (UVA) exposure, and a down-regulation of differentiation associated gene expression in response to violet light (Kim et al., 2013b; Wicks et al., 2011). The expression patterns of opsin genes and their role in regulating different biological processes suggest skin is a primary light responsive organ. Fish have dermal light receptors that have been shown regulated by physiological processes in skin. For example, pigment migration in Tilapia erythrophores is light wavelength dependent, presumably mediated by interactions between opsins and G proteins (Ban et al., 2005). The presence of dermal light responses suggests fish skin may serve as a model system to assess transcriptional responses to light.

Recently, we assessed the transcriptional effects of light exposure in fish skin using the *Xiphophorus* experimental model (Boswell et al., 2015; Chang et al., 2015; Lu et al., 2015; Walter et al., 2014; Walter et al., 2015; Yang et al., 2014). Walter et al. (2015). Exposure of

X. maculatus skin to 4,100 K FL resulted in suppression of at least 130 genes involved in chromosome segregation, cell cycle progression, and DNA replication/repair. Notably, in these studies, only a single time point (6 hrs) between FL exposure and RNA isolation was employed to assess subsequent gene expression changes. Thus, the FL post-exposure kinetics of transcriptional modulation in skin are not well characterized. Lack of knowledge regarding the kinetics of the light-induced gene expression responses hinders comparative investigation of differential transcriptional responses to varied FL sources and the ability to characterize the FL dose response.

To further investigate the transcriptional response elicited by FL exposure and characterize the post-exposure kinetics of the FL response on gene expression in fish skin, we exposed zebrafish (*Danio rerio*) to 4,100 K FL and utilized RNA-Seq to assess gene expression changes in skin 1 to 12 hrs after FL exposure. The time-dependent transcriptional responses obtained were functionally analyzed by collective assessment of the gene sets showing transcriptional modulation at each time point after FL exposure. We determined that FL exposure promoted both an early (1–2 hrs) robust response involving induction of genes associated with cell damage and cell proliferation as part of an overall immune/inflammatory response. We also show FL exposed zebrafish incite a protracted late (4–12 hrs) transcriptional response in gene sets predicted to maintain inflammation, as well as, transcriptional suppression of gene sets involved in lipid, xenobiotic, and melatonin metabolism.

Materials and Methods

Fish Utilized and Fluorescent Light Exposure

Adult zebrafish (Tu) used in this study were provided by the Zebrafish International Resource Center (ZIRC). Since zebrafish arrival, they were maintained under 10,000 K FL light in 14 hour/10 hour light/dark phases. All fishes used were mature 9-month-old males. This age was selected for two reasons: first of all, 9-month-old zebrafish were considered as fully developed young adults; second of all, this age is comparable to the age of other teleost fish species (i.e., *X. maculatus*) that were studied for light-incited genetic response. Prior to FL exposure, fish were individually placed in flasks containing 100 mL filtered aquaria water and put in the dark overnight (~12 hrs) and were not feed. Zebrafish were exposed in duplicate to 35 kJ/m^2 (40 min) of 4,100 K FL in a specially designed wooden box (77 cm × 41 cm × 36 cm) with a hinged wooden lid capable of sealing the interior of the box from external light. Fish were placed in UV transparent cuvettes (9 cm × 7.5 cm × 1.5 cm) in 70 mL of water. The exposure cuvettes were suspended 10 cm between two banks of two (total of 4 lights) “cool white” FL lamps (Philips, F20T-12/D, 4,100 K “cool white” lamps) mounted horizontally on each side of the wooden exposure chamber. The internal temperature was maintained at about 24 °C using 15.5 cm high speed fans located at the bottom ends of the wood box (Fig. 1b). The location where zebrafish used in this study were maintained receives 99.5 kJ/m^2 of light. 35 kJ/m^2 of FL exposure in the exposure chamber is equivalent to 295 minutes of FL exposure in animal housing condition. Unexposed control fish were dissected after the 12 hr dark period. Immediately after the 40 min exposure, all fish were returned to the dark for pre-determined dark incubation time points (1, 2, 4, 6, 8

10, or 12 hrs) before being euthanized and dissected for RNA isolation. All zebrafish were maintained and samples taken in accordance with protocol approved by IACUC (IACUC2015107711)

RNA Isolation and RNA-Seq

Fish were anesthetized by placing them on ice and sacrificed by cranial resection. Skin samples were immediately placed in 1.5 mL microcentrifuge tubes containing 300 μL TRI Reagent (Sigma Inc., St Louis, MO, USA) and flash frozen in an ethanol dry ice bath. Remaining tissues were placed in individual 1.5 mL microcentrifuge tubes with 300 μL RNA*later* (Life Technologies, Grand Island, NY, USA).

At each post exposure time point, RNA was isolated from skin using a TRI Reagent chloroform extraction followed by the Qiagen RNeasy RNA isolation protocol (Qiagen, Valencia, CA, USA). Briefly, skin samples were homogenized with a tissue homogenizer while frozen in TRI Reagent. After the initial homogenization, 300 μL of fresh TRI Reagent and 120 μL of chloroform were added to the 1.5 mL microcentrifuge tube and shaken vigorously for 15 sec. Phase separation was performed by centrifugation (12,000 × g for 5 min at 4 °C). The aqueous phase was then added to a new 1.5 mL microcentrifuge tube and an additional chloroform extraction was performed (300 μL TRI Reagent, 60 μL chloroform). Following extraction, the nucleic acids were precipitated with 500 μL of 70% EtOH and transferred to a Qiagen RNeasy mini spin column. DNase treatment was performed on-column for 15 min at 25 °C. RNA samples were subsequently eluted with 100 μL RNase free water. RNA concentration was measured using a Qubit 2.0 fluorometer (Life Technologies, Grand Island, NY, USA), RNA quality, RNA integrity (RIN) score, was assessed using an Agilent 2100 Bioanalyzer (Agilent Technologies, Santa Clara, Ca, USA). All samples sent for RNA-Seq had RIN scores ≥ 8.

RNA sequencing and raw reads filtering was performed as previously described (Boswell et al., 2015; Chang et al., 2015; Lu et al., 2015). Briefly, samples from each time point were sent in biological duplicates to Genewiz (Genewiz, South Plainfield, NJ, USA) for Illumina High-Throughput Sequencing (Illumina, Inc., San Diego, CA, USA). Individual sequencing libraries were constructed using the Illumina TruSeq mRNA Library Prep Kit with polyA selection, and libraries were sequenced (100 bp, paired-end [PE] reads) on the Illumina HiSeq 2000 platform. Sequencing adaptors were trimmed from raw reads, and subsequent short sequencing reads were filtered using a custom Perl script (Garcia et al., 2012) that removed low scoring sections of each read while preserving the longest remaining fragment (for statistics of RNA-Seq, Table 1).

Gene expression profiling and differential gene expression analysis

All processed reads were mapped to the zebrafish reference genome (GRCz10) using Tophat2 (Kim et al., 2013a). The percent of reads mapped and coverage was calculated by dividing total length of sequencing reads by length of the transcriptome (Table 1). Gene expression was quantified using FeatureCounts (Liao et al., 2014).

To assess overall variations of gene expression changes between two biological conditions, the distance between observed gene expression and a theoretical value that represents no differential expression between two biological conditions was calculated (Fig. 2b).

Differentially Expressed Genes (DEGs) between each time point after FL exposure compared to control were identified using R/Bioconductor edgeR package (Robinson et al., 2010). The Area Under Curve (AUC) of receiver operating characteristic curve was calculated to assess true and false positive rates for each gene tested. Coefficients of variance (CV) were calculated for library-size normalized read counts (CPM) of each gene separately in control or light exposed conditions. A set of statistical thresholds were applied to genes identified by edgeR to be DEGs: Log_2Fold Change (Log_2FC) ≥ 1 or −1, $Log_2CPM \geq 1$, False Discovery Rate (FDR) ≤ 0.01; AUC= 1; CV ≤ 0.5.

Functional analysis of differentially expressed genes

Zebrafish Ensemble gene IDs of DEGs were converted to human homolog gene IDs using Ensemble Biomart. Functional analysis of DEGs was performed using Ingenuity Pathway Analysis (IPA; Qiagen, Redwood City, CA.) for clustering and assessing effected genetic pathways represented by DEGs. Herein, the term “pathways” is short for canonical pathways as assigned by IPA based on input DEG data. IPA assigns DEGs to pathways if the analysis results in a DEG that has previously been identified within well-established signaling or metabolic pathways based on published literature. Pathway analysis is performed by testing the over-representation of genes belonging to a certain pathway in the input DEGs. Pathways with an enrichment $-\log_{10}(p\text{-value})$ score > 1.3 (p-value < 0.05) were kept for further analysis. Pathway for the early response were determined by the combined DEGs from 1 and 2 hr time points, and pathway for the late response were determined by the combined DEGs between 4–12 hr time points that were present in at least two of the five time points.

Validation of RNA-Seq by Quantitative Real Time PCR

Quantitative Real Time PCR (qRT-PCR) was performed as previously described (Walter et al., 2014). Briefly, RNA from isolated skin samples was converted to cDNA using a High Capacity cDNA Reverse Transcription Kit (Applied Biosystems, Foster City, CA, USA) following the manufactures instructions. Synthesized cDNA was used in qRT-PCR SYBR Green-based-detection methods on an Applied Biosystems 7500 Fast System (Applied Biosystems, Carlsbad, CA, USA) for all qRT-PCR reactions. Primers were designed using Geneious (Biomatters Ltd, Auckland, New Zealand) bioinformatics software. All primers designed had 40–60% GC content and a T_m between 60–62 °C with less than 1 °C difference within each primer set. Primer lengths were designed to be 18–26 bp and cross at least one exon-exon junction, and amplicon size was between 70–200 bp long. The efficiency of all primers was tested in triplicate 20 μL reactions in a standard serial dilution series of 100, 10, 1, 0.1 ng cDNA. Primers specific for the zebrafish transcripts (Supplemental Table 3) were tested for efficiency, and only primers with efficiency values between 70–120% were selected for gene expression analysis.

Two biological replicates with 4 technical replicates of each sample were plated for expression analysis. Fold change expression relative to unexposed skin samples was

determined, and 18S rRNA was used as a normalization transcript for all samples. mRNA expressions relative to the 18S rRNA endogenous control were calculated by applying $2^{-\Delta CT}$. Calculated values represent the mRNA expression level for each target tested relative to the 18S rRNA control. Fold change for each sample was determined relative to each respective unexposed control sample and standard deviations were calculated for the average of 4 technical replicates.

Results

Gene expression variance at different time points following FL exposure

After exposure to 35 kJ/m^2 of 4,100 K FL, zebrafish were placed in the dark for pre-defined times (1, 2, 4, 6, 8, 10 or 12 hrs) to allow time for modulation of gene expression profiles in the skin (Fig. 2a). To assess the overall gene expression changes, we compared transcription between any two of the times post-exposure (Fig. 2b, c, d). Based on the variance of gene expression between control and each post-exposure time point, the largest transcriptional effect was found at 1 hr post-exposure, followed with 2 hrs post-exposure, and the variance decreased as post-exposure time increased (Fig. 2c, top row). Similarly, when comparing the variation in gene expression between any two neighboring time points (e.g., control vs. 1hr, 1 hr vs. 2 hr, etc.), the variation also appears lower after 4 hrs (i.e., 4–12 hrs), and higher within the first 2 hrs of FL exposure (control and 1 hr, 1 and 2 hrs; Fig. 2c). Quantification of gene expression variance supports this observation as gene expression variance is largest between control and 1hr, and between control and 2hr, after FL exposure and decreases from 4 hrs after FL exposure (Fig. 2d).

Kinetics of differential gene expression after FL exposure

We assessed DEGs for each time point following FL exposure. At 1 and 2 hrs after FL exposure, 835 (608 up-regulated, 227 down-regulated) and 1,102 (557 up-regulated, 545 down-regulated) DEGs were observed, respectively (Fig. 3a). At 4 to 12 hrs post-exposure, the number of DEGs decreased to 82 at 4 hrs (40 up-regulated, 42 down-regulated), 76 at 6 hrs (25 up-regulated, 51 down-regulated), 108 at 8 hrs (46 up-regulated, 62 down-regulated), 178 at 10 hrs (55 up-regulated, 123 down-regulated) and 77 at 12 hrs (12 up-regulated, 65 down-regulated, Fig. 3a). Thus, the numbers of DEGs reflect the trend in overall gene expression variance (Fig. 2, 3a). Two hours after FL exposure the largest number of DEGs is observed. Additionally, changes in gene expression (i.e., $\log_2$FC) also tend to be larger in the first two hours than at the other time points (Fig. 3b).

Functional analysis of the FL transcriptional response

The identified DEGs serve as markers representing the expression variance incited by FL, and thus were further analyzed. Since analysis of overall gene expression variance, and identification of specific DEGs, showed a decrease in the degree of gene expression change from 4 hrs post FL exposure (Fig. 2, 3), we designated the 1 and 2 hr DEGs as an “early” gene expression response in skin, while the 4 to 12 hr DEGs are designated the “late” gene expression response.

Functional analysis of the early genetic response identified 17 canonical pathways (Table 2) related to cell-microenvironment interaction (5 pathways), inflammation (5 pathways), cell proliferation (5 pathways) and lipid regulation (2 pathways; Table 2). However, pathways within different cell functions include genes involved in several signaling pathways that are interconnected (Table 2).

In contrast, functional analysis of DEGs comprising the late transcriptional response identified 10 canonical signaling pathways belonging to 2 major cellular functions; up-modulation of inflammation associated genes and concurrent suppression of genes associated with cholesterol/lipid, xenobiotic and melatonin metabolism, and suppression of LPS/IL-1 mediated inhibition of retinoid X receptor (i.e., RXR) function (Table 2). The late response maintains the induction of inflammation associated genes over 12 hrs. However, late response related inflammation genes appear to serve a different function in the inflammation process than those in the early response (Table 2).

Validation of RNA-Seq gene expression changes using qRT-PCR in zebrafish skin

As a technical validation, qRT-PCR was utilized to assess the expression changes of 7 DEGs (*cebpb, papss2a, hsp70l, cry7a1, fosab, myh7ba, il1b*) identified at different time points using RNA-Seq. The expression change (i.e., fold change) between different time points and control assessed by RNA-Seq was compared to the qRT-PCR fold changes. Among the 42 qRT-PCR assays performed, the direction of gene expression change (i.e., up-regulation or down-regulation) for 38 assays (90.5%) were consistent with the RNA-Seq results (Fig. 4).

Discussion

Evolution occurred exclusively under the full spectrum of sunlight (Fig. 1a; Judson, 2017). Therefore, all spectral wavelengths were present and potentially utilized in cellular photoreception mechanisms over the course of vertebrate evolution. In contrast, FL has been in service for only about 60 years, and has an emission spectrum that is considerably different than the solar spectrum. FL emits a much narrower and less complex set of wavelengths than the sun. Since gene expression patterns evolved in response to solar spectrum, one may surmise the spectrally less complex artificial light may not produce all signals available to photoreceptors, and this could result in altered transcription and/or cellular functions. However, the effects of artificial light exposure on gene expression in animals have only recently begun to be investigated. Exposure of *X. maculatus* to 4,100 K FL is reported to result in transcriptional suppression of at least 130 genes involved in chromosome segregation, cell cycle progression, and DNA replication/repair in skin (Walter et al., 2015). Further, it has been shown that exposure of *X. maculatus* to specific 50 nm light wavebands produces waveband specific transcriptional effects on unique sets of genes in skin (Chang et al., 2015). These early studies employed a post-exposure time of 6 hrs to allow transcriptional remodeling to occur. The experimental results reported herein characterize the post-exposure kinetics of differential gene expression over a 12 hr period in zebrafish skin after exposure to the commonly used FL source (i.e., 4,100 K, or “cool white” light).

In this study, FL exposure resulted in a genetic response consisting of two phases, an early response occurring within 1 hr and lasting at least 2 hrs post-exposure, and a late response that is maintained up to 12 hrs after the FL exposure. Both the overall variance in gene expression and numbers of transcriptional DEGs occurred 1 to 2 hrs after FL exposure are larger than the rest of the post-exposure time points (Figs. 2, 3). There were more up-regulated genes in the early response after FL exposure (Fig. 3a) and these DEGs exhibited a larger dynamic range of expression change (Fig. 3b). The differences in scale between early and late FL transcriptional responses may suggest different mechanisms are regulating different phases. In the early phase, the robust genetic response may be a result of enhanced transcription of genes already active at a basal level combined with selective degradation of mRNA that is not derived from “light responsive” genes. For example, it has been shown that light responsive miR-183 controls the rapid elevation of *e4bp4-6* expression between 1 and 2 hrs after light exposure (Ben-Moshe et al., 2014). We speculate such mechanisms may be very common and could provide the rapid and robust transcriptional response observed in the early phase genetic response.

The early genetic response consists of an interconnected network of signaling pathways involved in cell-microenvironment interactions, inflammation, cell proliferation and lipid regulation (Table 2, Fig. 5). Cell proliferation related genes consist of up- and down-regulated genes that are known to be controlled by major pro-proliferation pathway regulators (Table 2; Fig. 5). Down-regulation of pik3r2 and braf indicate both PI3K-Akt signaling and MAPK signaling is repressed. However, myc, vegfa, hif1a, and mapk6 were up-regulated. The observed antagonistic genetic changes suggest certain proliferative pathways (e.g., HIF1-VEGF pathway, PI3K signaling down-stream pathway, MAPK signaling down-stream pathway) are alternatively activated by FL exposure. Transcriptionally up-regulated genes involved with cell-microenvironment interactions suggest infiltration of immune cells may be a part of the overall inflammatory response. It has been reported that intense ocular light exposure leads to photoreceptor degradation in the retina through inflammatory pathways (Bian et al., 2016; Song et al., 2016). Judging from the genetic response associated with inflammation and proliferation, we speculate similar light-initiated cellular damage also occurs in extraocular organs (e.g., skin).

The signaling pathways related to cell proliferation and cell-microenvironment interactions are absent in the late phase FL response. However, genes associated with inflammation related pathways continued to show up-regulated. Compared to other fish models used in biomedical research, FL appears to up-regulate inflammatory and immune responses in both medaka and zebrafish. In contrast, platyfish show suppression of the immune response and genes associated with cell cycle progression 6 hr after FL exposure (another manuscript in this edition). In contrast to the early phase, inflammation associated genes that are transcriptionally activated are primarily chemokines, indicative of the longer-term later response to FL exposure (Fig. 5). Another cluster of FL transcriptionally responsive genes in the late phase response are involved in lipid and cholesterol metabolism, as well as, detoxification enzymes (Table 2, Fig. 5). Down-regulation of cholesterol metabolism related genes is associated with elevated cholesterol levels in human inflamed skin (i.e., psoriatic lesions), and is triggered by interleukin signaling (i.e., IL-17A signaling; Varshney et al., 2016). Though we did not observe interleukin signaling to be directly activated upon FL

exposure, the up-regulation of chemokines (i.e., *cxcl*) in the late phase FL response is consistent with interleukin pathway activation (Cua and Tato, 2010; Harper et al., 2009; Shen et al., 2006). Therefore, transcriptional repression of cholesterol metabolism, as well as other metabolic genes, is likely a result of secondary effects of up-regulation of inflammation associated genes, and supports immune cell infiltration observed in the early phase response (Fig. 5).

As stated earlier, FL doesn't represent sunlight spectrum. This raises the question of whether and how FL incited genetic response is different from sunlight. However, full spectrum sunlight genetic response is not well studied due to the uncontrollable intensity variance in different geological location, altitude, season etc. In contrast, genetic response to UV radiation is well studied. It has been shown that inflammatory response and change in lipid metabolism are associated with UV exposure in both human and fish (i.e., platyfish) skin (Boswell et al., 2015; Yang et al., 2014; McGrath et al., 2012; Nicolaou et al., 2011; Aoki et al., 2007; Kuhn et al., 2006; Brink et al., 2000). Consider these functional similarity, it suggests that FL and UV radiation have similar effect in terms of inflammation induction and affect lipid metabolism. Therefore prolonged exposure to FL, especially at circadian dark phase, may pose excessive damage that not allowing organism to repair, and lead to chronic disorders.

In summary, these results establish transcriptional modulation in FL exposed zebrafish skin to exhibit post-exposure time-dependent genetic responses characterized by an acute early phase and a protracted late phase, each involving unique gene sets. After FL exposure, cell damage, coupled with immune cell migration/infiltration (i.e., inflammation) occurs rapidly (i.e., within 1 hr). This initial response transitions to a late phase immune response at some point after 2 hrs and remains activated through 12 hrs. The late phase response is likely a result of interactions between immune cells and inflamed skin, as well as changes in secondary metabolic pathways as a result of inflammation.

Conclusion

We have characterized the kinetics of the transcriptional response to FL exposure in zebrafish skin and conclude that FL exposure induced interrelated early and late phases of an inflammatory response, with each phase involving different mechanisms and associated genes. Gene expression and functional analyses suggests the early response is involved with the perception of photo-damage in the skin and the infiltration of immune cells, while the late response is a functional continuation of the early genetic phase, that includes a cytokine regulated cellular response to inflammation.

Supplementary Material

Refer to Web version on PubMed Central for supplementary material.

Acknowledgments

The authors would like to thank the staff of the *Xiphophorus* Genetic Stock Center, Texas State University, for maintaining the fish and caring for the animals used in this study. Support for this project was provided in part by the NIH grant awards; R25-GM-102783, R25-GM-107759, R24-OD-011120, R24-OD-018555.

Funding: This work was supported by the National Institutes of Health, R25-GM-102783, R25-GM-107759, R24-OD-011120, R24-OD-018555

References

Aoki H, Moro O, Tagami H, Kishimoto J. Gene expression profiling analysis of solar lentigo in relation to immunohistochemical characteristics. Br J Dermatol. 2007; 156:1214–1223. [PubMed: 17419692]

Ban E, Kasai A, Sato M, Yokozeki A, Hisatomi O, Oshima N. The signaling pathway in photoresponses that may be mediated by visual pigments in erythrophores of Nile tilapia. Pigment Cell Res. 2005; 18:360–369. [PubMed: 16162176]

Ben-Moshe Z, Alon S, Mracek P, Faigenbloom L, Tovin A, Vatine GD, Eisenberg E, Foulkes NS, Gothilf Y. The light-induced transcriptome of the zebrafish pineal gland reveals complex regulation of the circadian clockwork by light. Nucleic Acids Res. 2014; 42:3750–3767. [PubMed: 24423866]

Bian M, Du X, Cui J, Wang P, Wang W, Zhu W, Zhang T, Chen Y. Celastrol protects mouse retinas from bright light-induced degeneration through inhibition of oxidative stress and inflammation. J Neuroinflammation. 2016; 13:50. [PubMed: 26920853]

Blask DE. Melatonin, sleep disturbance and cancer risk. Sleep Med Rev. 2009; 13:257–264. [PubMed: 19095474]

Blask DE, Brainard GC, Dauchy RT, Hanifin JP, Davidson LK, Krause JA, Sauer LA, Rivera-Bermudez MA, Dubocovich ML, Jasser SA, Lynch DT, Rollag MD, Zalatan F. Melatonin-depleted blood from premenopausal women exposed to light at night stimulates growth of human breast cancer xenografts in nude rats. Cancer Res. 2005; 65:11174–11184. [PubMed: 16322268]

Brink N, Szamel M, Young AR, Wittern KP, Bergemann J. Comparative quantification of IL-1beta, IL-10, IL-10r, TNFalpha and IL-7 mRNA levels in UV-irradiated human skin in vivo. Inflamm Res. 2000; 49:290–296. [PubMed: 10939619]

Boswell W, Boswell M, Titus J, Savage M, Lu Y, Shen J, Walter RB. Sex-specific molecular genetic response to UVB exposure in Xiphophorus maculatus skin. Comp Biochem Physiol C Toxicol Pharmacol. 2015; 178:76–85. [PubMed: 26256120]

Brainard GC, Lewy J, Menaker M, Fredrickson RH, Miller LS, Weleber RG, Cassone V, Hudson D. Effect of Light Wavelength on the Suppression of Nocturnal Plasma Melatonin in Normal Volunteers. annals of the new york academy of sciences. 1985; 453:376–378.

Cajochen C, Munch M, Kobialka S, Krauchi K, Steiner R, Oelhafen P, Orgul S, Wirz-Justice A. High sensitivity of human melatonin, alertness, thermoregulation, and heart rate to short wavelength light. J Clin Endocrinol Metab. 2005; 90:1311–1316. [PubMed: 15585546]

Chang J, Lu Y, Boswell WT, Boswell M, Caballero KL, Walter RB. Molecular genetic response to varied wavelengths of light in Xiphophorus maculatus skin. Comp Biochem Physiol C Toxicol Pharmacol. 2015; 178:104–115. [PubMed: 26460196]

Contreras AJ, Boswell M, Downs KP, Pasquali A, Walter RB. Cortisol release in response to UVB exposure in Xiphophorus fish. Comp Biochem Physiol C Toxicol Pharmacol. 2014; 163:95–101. [PubMed: 24625568]

Cua DJ, Tato CM. Innate IL-17-producing cells: the sentinels of the immune system. Nat Rev Immunol. 2010; 10:479–489. [PubMed: 20559326]

Garcia TI, Shen Y, Catchen J, Amores A, Schartl M, Postlethwait J, Walter RB. Effects of short read quality and quantity on a *de novo* vertebrate transcriptome assembly. Comp Biochem Physiol C Toxicol Pharmacol. 2012; 155:95–101. [PubMed: 21651990]

Haltaufderhyde K, Ozdeslik RN, Wicks NL, Najera JA, Oancea E. Opsin expression in human epidermal skin. Photochem Photobiol. 2015; 91:117–123. [PubMed: 25267311]

Harper EG, Guo C, Rizzo H, Lillis JV, Kurtz SE, Skorcheva I, Purdy D, Fitch E, Iordanov M, Blauvelt A. Th17 cytokines stimulate CCL20 expression in keratinocytes in vitro and in vivo: implications for psoriasis pathogenesis. J Invest Dermatol. 2009; 129:2175–2183. [PubMed: 19295614]

Holick MF. Vitamin D and bone health. J Nutr. 1996; 126:1159S–1164S. [PubMed: 8642450]

Judson OP. The energy expansions of evolution. Nat Ecol Evol. 2017; 1:138. [PubMed: 28812646]

Kim D, Pertea G, Trapnell C, Pimentel H, Kelley R, Salzberg SL. TopHat2: accurate alignment of transcriptomes in the presence of insertions, deletions and gene fusions. Genome Biol. 2013a; 14:R36. [PubMed: 23618408]

Kim HJ, Son ED, Jung JY, Choi H, Lee TR, Shin DW. Violet light down-regulates the expression of specific differentiation markers through Rhodopsin in normal human epidermal keratinocytes. PLoS One. 2013b; 8:e73678. [PubMed: 24069221]

Kojima D, Mori S, Torii M, Wada A, Morishita R, Fukada Y. UV-sensitive photoreceptor protein OPN5 in humans and mice. PLoS One. 2011; 6:e26388. [PubMed: 22043319]

Koo YS, Song JY, Joo EY, Lee HJ, Lee E, Lee SK, Jung KY. Outdoor artificial light at night, obesity, and sleep health: Cross-sectional analysis in the KoGES study. Chronobiol Int. 2016; 33:301–314. [PubMed: 26950542]

Kuhn M, Wolber R, Kolbe L, Schnorr O, Sies H. Solar-simulated radiation induces secretion of IL-6 and production of isoprostanes in human skin in vivo. Arch Dermatol Res. 2006; 297:477–479. [PubMed: 16491351]

Leung NY, Montell C. Unconventional Roles of Opsins. Annu Rev Cell Dev Biol. 2017

Lewy AJ, Wehr TA, Goodwin FK, Newsome DA, Markey SP. Light suppresses melatonin secretion in humans. Science. 1980; 210:1267–1269. [PubMed: 7434030]

Liao Y, Smyth GK, Shi W. featureCounts: an efficient general purpose program for assigning sequence reads to genomic features. Bioinformatics. 2014; 30:923–930. [PubMed: 24227677]

Lu Y, Bowswell M, Bowswell W, Yang K, Schartl M, Walter RB. Molecular genetic response of Xiphophorus maculatus-X. couchianus interspecies hybrid skin to UVB exposure. Comp Biochem Physiol C Toxicol Pharmacol. 2015; 178:86–92. [PubMed: 26254713]

Lucassen EA, Coomans CP, van Putten M, de Kreij SR, van Genugten JH, Sutorius RP, de Rooij KE, van der Velde M, Verhoeve SL, Smit JW, Lowik CW, Smits HH, Guigas B, Aartsma-Rus AM, Meijer JH. Environmental 24-hr Cycles Are Essential for Health. Curr Biol. 2016; 26:1843–1853. [PubMed: 27426518]

McColl SL, Veitch JA. Full-spectrum fluorescent lighting: a review of its effects on physiology and health. Psychol Med. 2001; 31:949–964. [PubMed: 11513381]

McGrath JA, Robinson MK, Binder RL. Skin differences based on age and chronicity of ultraviolet exposure: results from a gene expression profiling study. Br J Dermatol. 2012; 166(Suppl 2):9–15. [PubMed: 22670613]

Nicolaou A, Pilkington SM, Rhodes LE. Ultraviolet-radiation induced skin inflammation: dissecting the role of bioactive lipids. Chem Phys Lipids. 2011; 164:535–543. [PubMed: 21524643]

Ohayon MM, Milesi C. Artificial Outdoor Nighttime Lights Associate with Altered Sleep Behavior in the American General Population. Sleep. 2016; 39:1311–1320. [PubMed: 27091523]

Robinson MD, McCarthy DJ, Smyth GK. edgeR: a Bioconductor package for differential expression analysis of digital gene expression data. Bioinformatics. 2010; 26:139–140. [PubMed: 19910308]

Romeo S, Vitale F, Viaggi C, di Marco S, Aloisi G, Fasciani I, Pardini C, Pietrantoni I, Di Paolo M, Riccitelli S, Maccarone R, Mattei C, Capannolo M, Rossi M, Capozzo A, Corsini GU, Scarnati E, Lozzi L, Vaglini F, Maggio R. Fluorescent light induces neurodegeneration in the rodent nigrostriatal system but near infrared LED light does not. Brain Res. 2017; 1662:87–101. [PubMed: 28263713]

Schwimmer H, Metzer A, Pilosof Y, Szyf M, Machnes ZM, Fares F, Harel O, Haim A. Light at night and melatonin have opposite effects on breast cancer tumors in mice assessed by growth rates and global DNA methylation. Chronobiol Int. 2014; 31:144–150. [PubMed: 24131150]

Shen F, Hu Z, Goswami J, Gaffen SL. Identification of common transcriptional regulatory elements in interleukin-17 target genes. J Biol Chem. 2006; 281:24138–24148. [PubMed: 16798734]

Song D, Song J, Wang C, Li Y, Dunaief JL. Berberine protects against light-induced photoreceptor degeneration in the mouse retina. Exp Eye Res. 2016; 145:1–9. [PubMed: 26475979]

Stevens RG, Brainard GC, Blask DE, Lockley SW, Motta ME. Adverse health effects of nighttime lighting: comments on American Medical Association policy statement. Am J Prev Med. 2013; 45:343–346. [PubMed: 23953362]

Thapan K, Arendt J, Skene DJ. An action spectrum for melatonin suppression: evidence for a novel non-rod, non-cone photoreceptor system in humans. J Physiol. 2001; 535:261–267. [PubMed: 11507175]

Tsutsumi M, Ikeyama K, Denda S, Nakanishi J, Fuziwara S, Aoki H, Denda M. Expressions of rod and cone photoreceptor-like proteins in human epidermis. Exp Dermatol. 2009; 18:567–570. [PubMed: 19493002]

Varshney P, Narasimhan A, Mittal S, Malik G, Sardana K, Saini N. Transcriptome profiling unveils the role of cholesterol in IL-17A signaling in psoriasis. Sci Rep. 2016; 6:19295. [PubMed: 26781963]

Walter DJ, Boswell M, Volk de Garcia SM, Walter SM, Breitenfeldt EW, Boswell W, Walter RB. Characterization and differential expression of CPD and 6-4 DNA photolyases in Xiphophorus species and interspecies hybrids. Comp Biochem Physiol C Toxicol Pharmacol. 2014; 163:77–85. [PubMed: 24496042]

Walter RB, Walter DJ, Boswell WT, Caballero KL, Boswell M, Lu Y, Chang J, Savage MG. Exposure to fluorescent light triggers down regulation of genes involved with mitotic progression in Xiphophorus skin. Comp Biochem Physiol C Toxicol Pharmacol. 2015; 178:93–103. [PubMed: 26334372]

Wicks NL, Chan JW, Najera JA, Ciriello JM, Oancea E. UVA phototransduction drives early melanin synthesis in human melanocytes. Curr Biol. 2011; 21:1906–1911. [PubMed: 22055294]

Wurtman RJ. The effects of light on man and other mammals. Annu Rev Physiol. 1975a; 37:467–483. [PubMed: 1092254]

Wurtman RJ. The effects of light on the human body. Sci Am. 1975b; 233:69–77. [PubMed: 1145170]

Yang K, Boswell M, Walter DJ, Downs KP, Gaston-Pravia K, Garcia T, Shen Y, Mitchell DL, Walter RB. UVB-induced gene expression in the skin of Xiphophorus maculatus Jp 163 B. Comp Biochem Physiol C Toxicol Pharmacol. 2014; 163:86–94. [PubMed: 24556253]

(a)

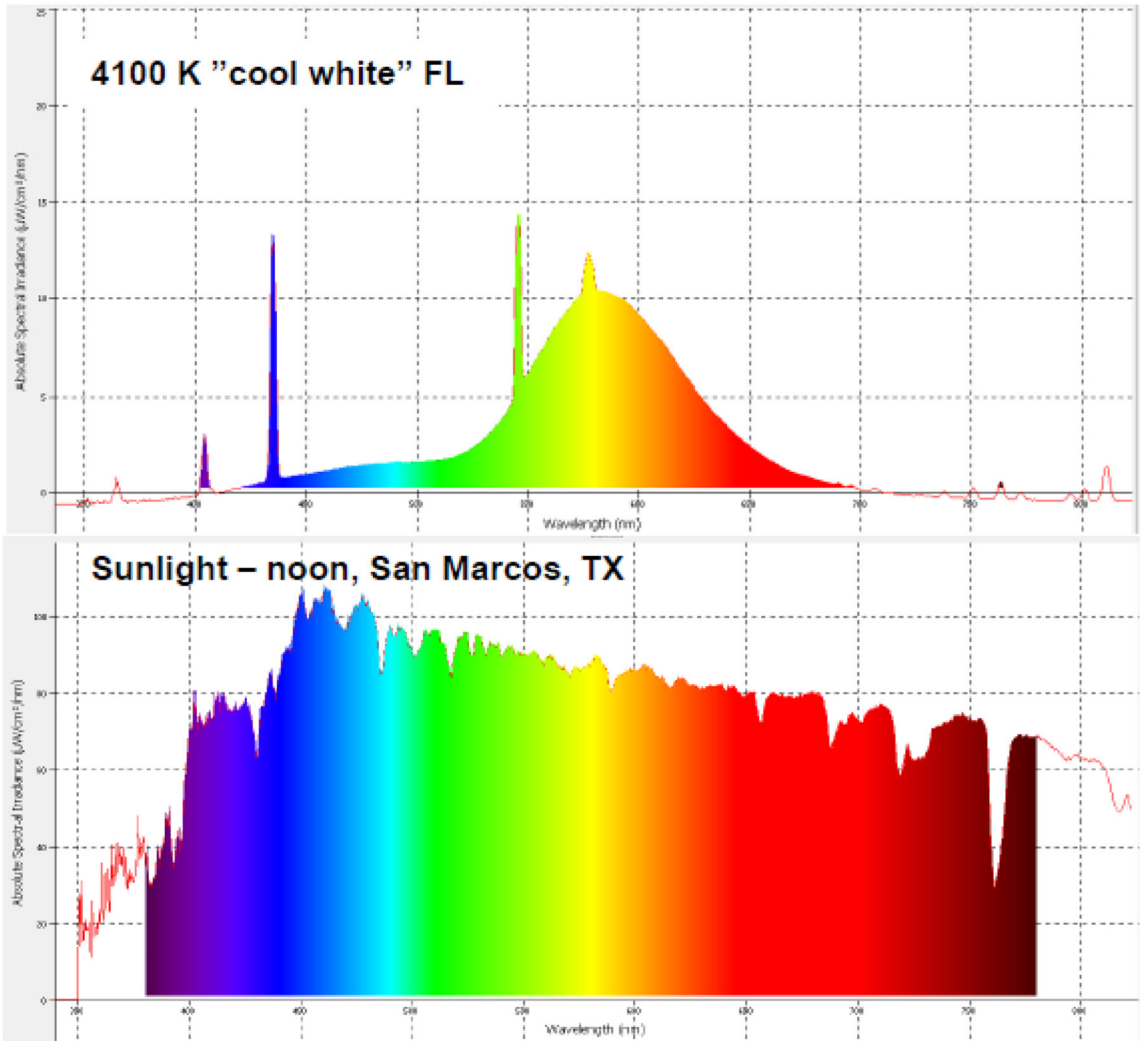

(b)

Figure 1. Spectrum of sunlight and 4,100 K FL

(a) Complex spectra for 4,100 K FL (top) or solar light measured at noon in San Marcos, TX, USA (bottom). Increments on x axis are 50 nm. (b) A specially designed wooden box (77 cm × 41 cm × 36 cm), with a hinged wooden lid capable of sealing the interior of the box from external light, is used for 4,100 K FL exposure. The exposure box is equipped with two banks of two (total of 4 lights) “cool white” FL lamps (Philips, F20T-12/D, 4,100 K “cool white” lamps) mounted horizontally on each side. The internal temperature is maintained at about 24 °C using 15.5 cm high speed fans located at the bottom ends of the wood box

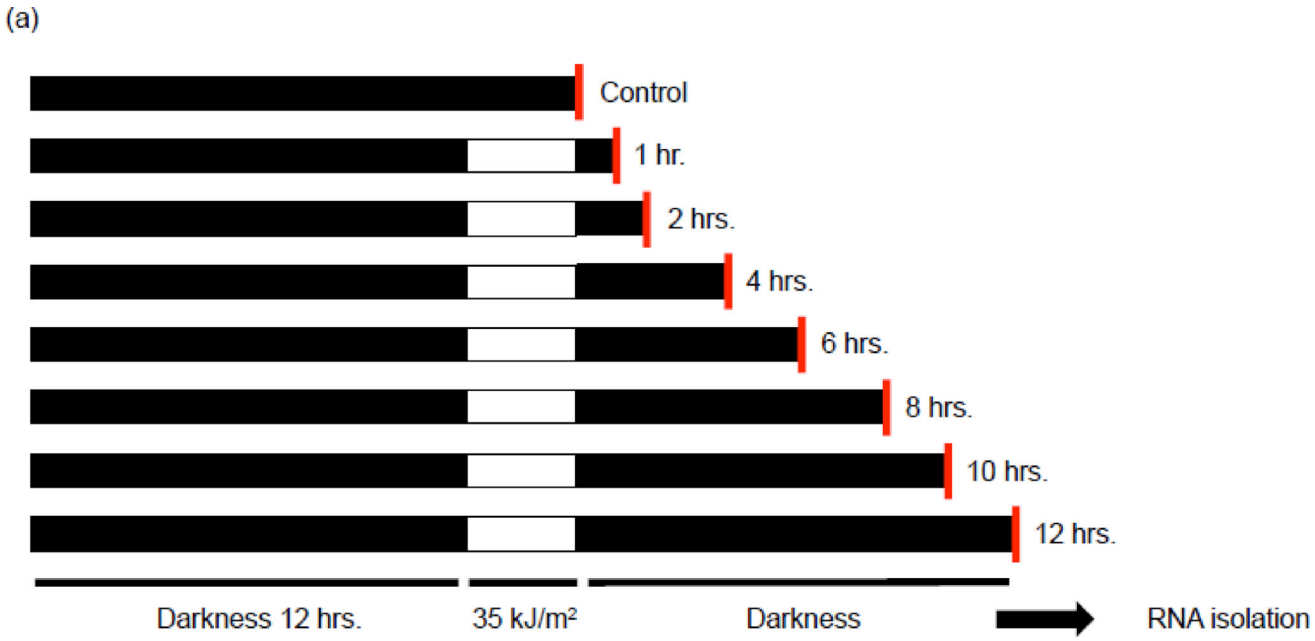

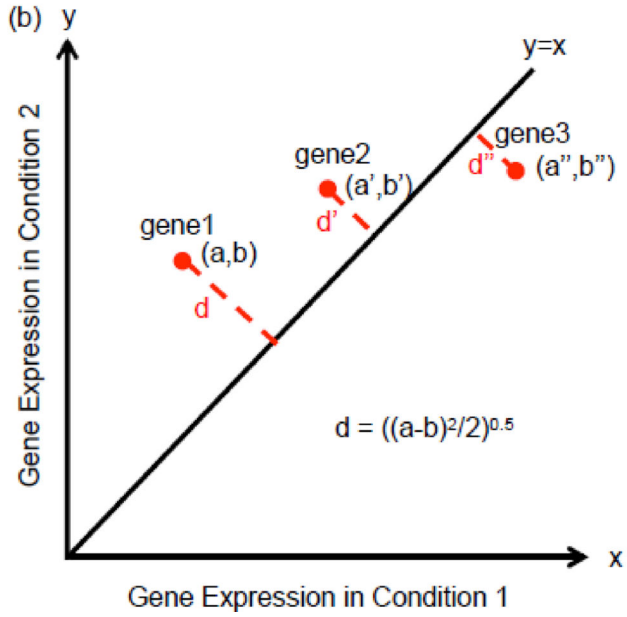

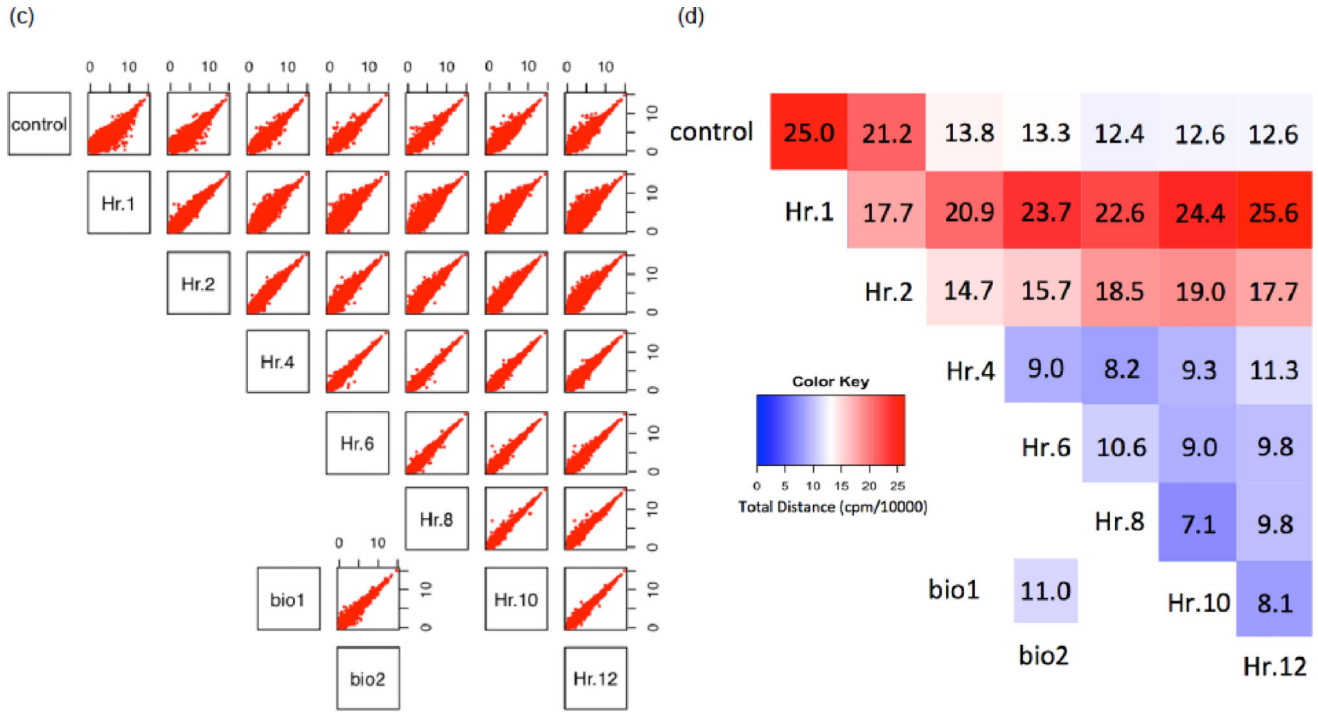

Figure 2. Gene Expression in zebrafish skin

(a) Experimental overview. (b) Quantification of gene expression variance between two conditions. The x and y axis represent gene expression in condition 1 and 2, respectively. In each sub-plot, the number on the x and y axis represent normalized and $\log_2$ transformed gene expression values. The more similar the two conditions are to each other, the narrower the region that gene expression plot will fall into, and the closer the data distribution is to a central line (y=x) which represents no genetic change, and the less variable the gene expression profiles are to each other. To quantify the variance in gene expression between two conditions, the distance "d" between any gene and the line y=x was calculated using $d=((a-b)^2/2)^{0.5}$. (c) Gene expression plot between two biological conditions are presented as dot plots. Control indicates unexposed fish and bio1 and 2 represent each of the two control biological replicates. Each dot represents one gene. The x and y coordinates of each dot are the expression values in two different conditions. (d) Quantification of differences between two biological conditions was calculated as described in (b). The color and numerical value of each color block represents the total distance of gene expression from the y=x line.

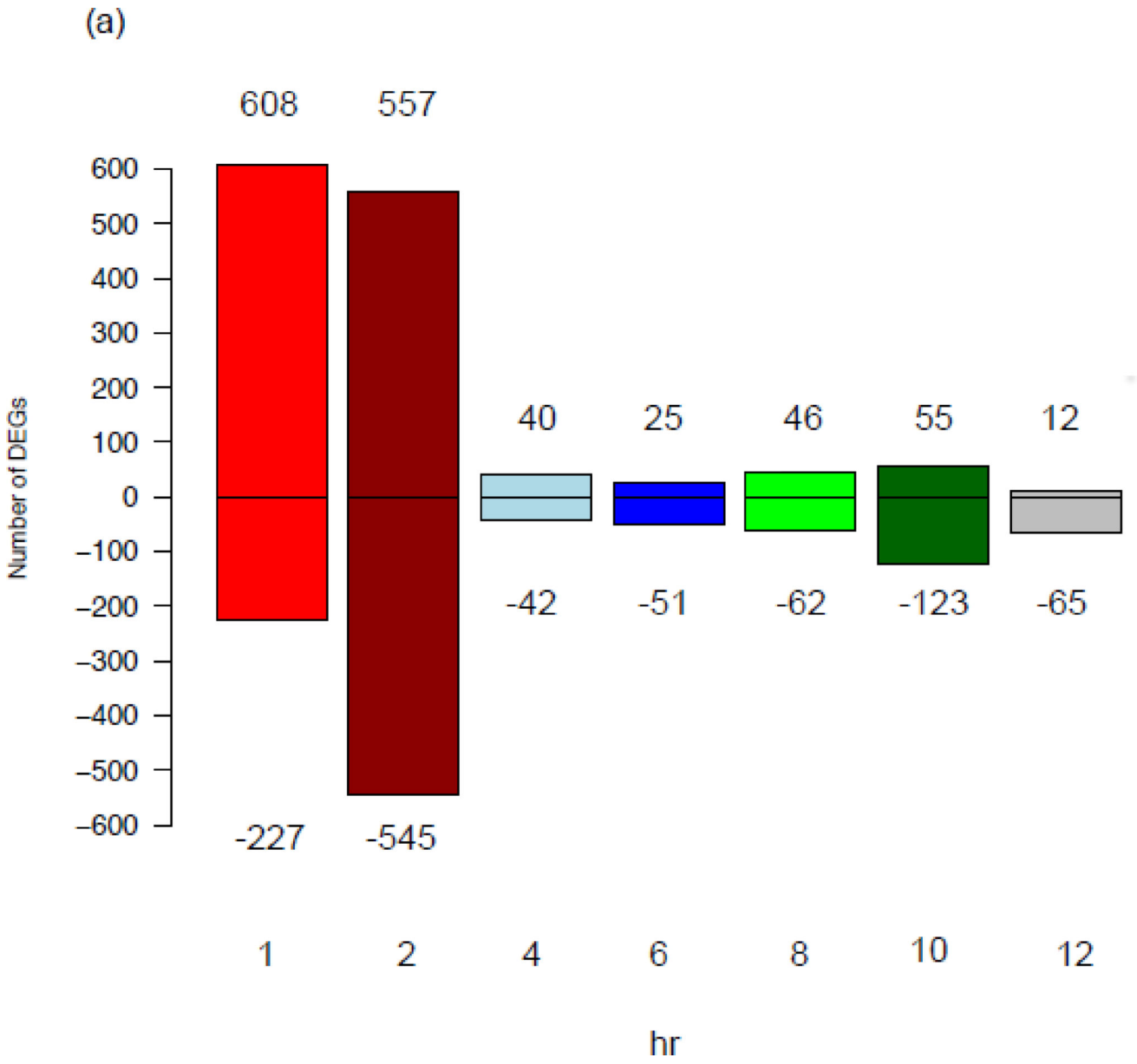

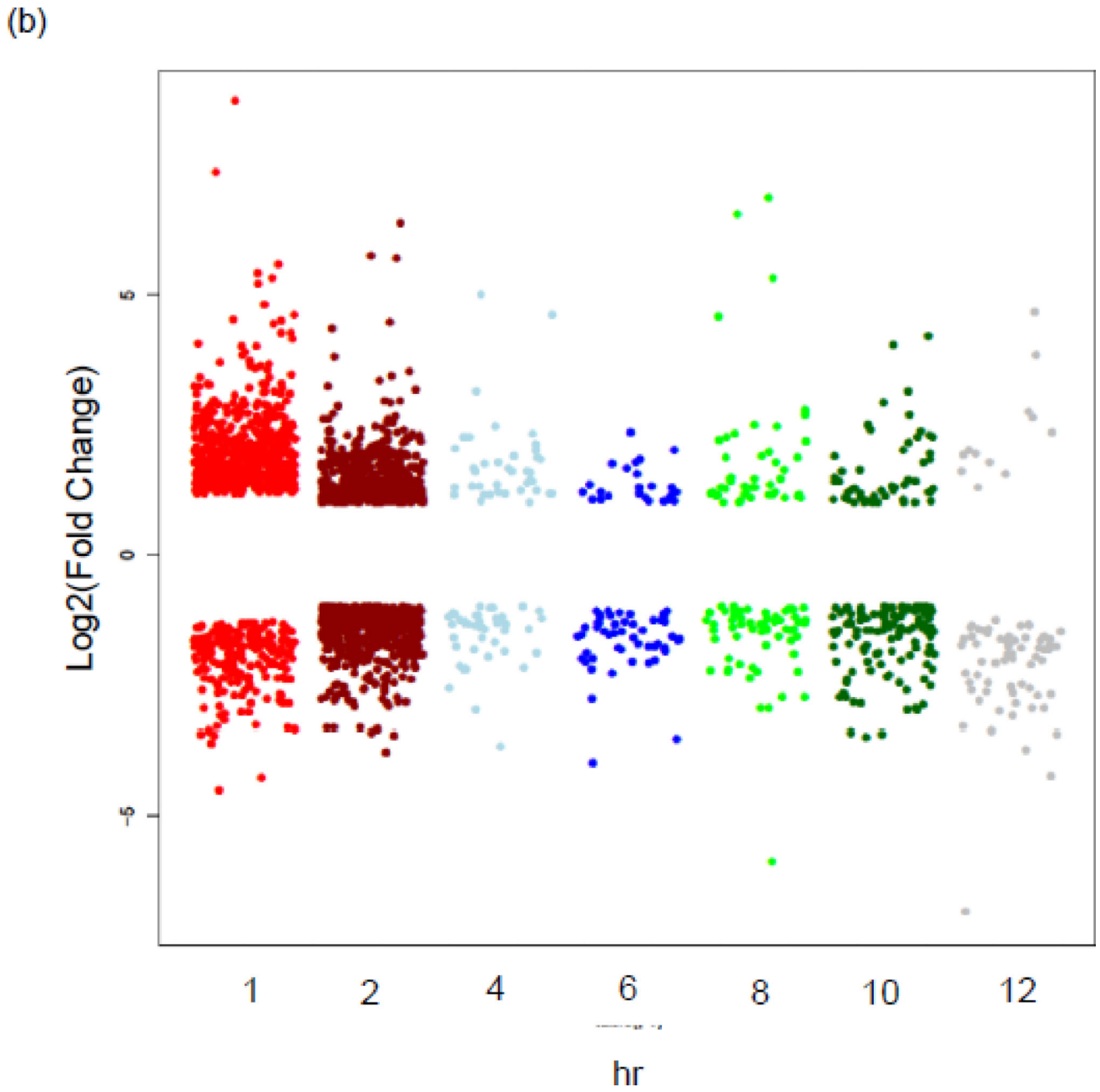

Figure 3. Differential gene expression in zebrafish skin

(a) Differentially expressed genes (DEGs) for various lengths of dark incubations compared to unexposed control in zebrafish skin following 35 kJ/m^2 of 4,100 K FL exposure. DEGs are determined by Log_2Fold Change ≥1 or ≤−1, Log_2CPM ≥1, False Discovery Rate ≤0.01, AUC =1; Coefficients of variance ≤0.5. (b) Genetic response of DEGs at each time point. Each dot represents one DEG at a certain time point.

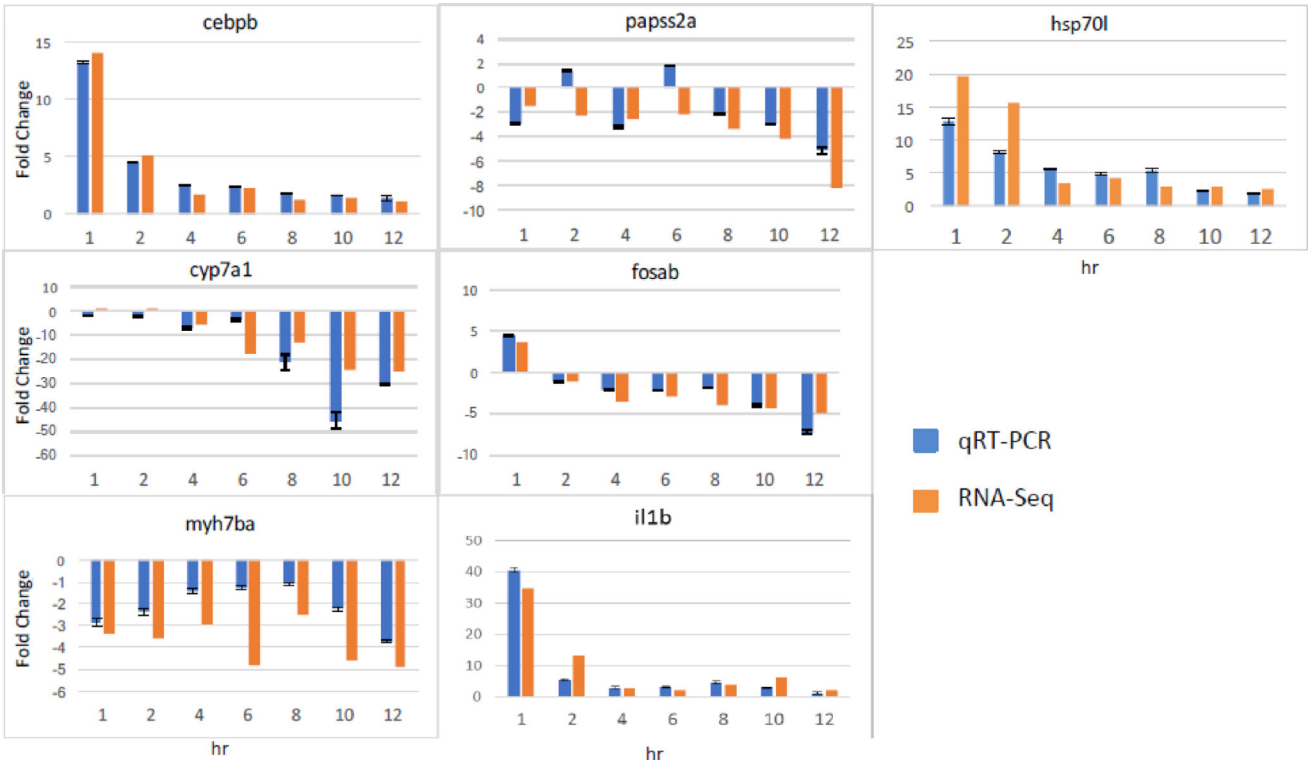

Figure 4. Validation of RNA-Seq gene expression changes using qRT-PCR in zebrafish skin

Seven DEGs identified at different time points following 35 kJ/m^2 FL exposure by RNA-Seq are confirmed using qRT-PCR. Concentration of target mRNA was first normalized to 18S rRNA, and subsequently compared to expression of that in unexposed fish to determine fold change. In each graph, values along x-axis represent length of time after FL exposure; values along y axis represent fold change at each post-exposure time point. At each time point, blue bar represents qPCR result, and orange bar represents RNA-Seq result.

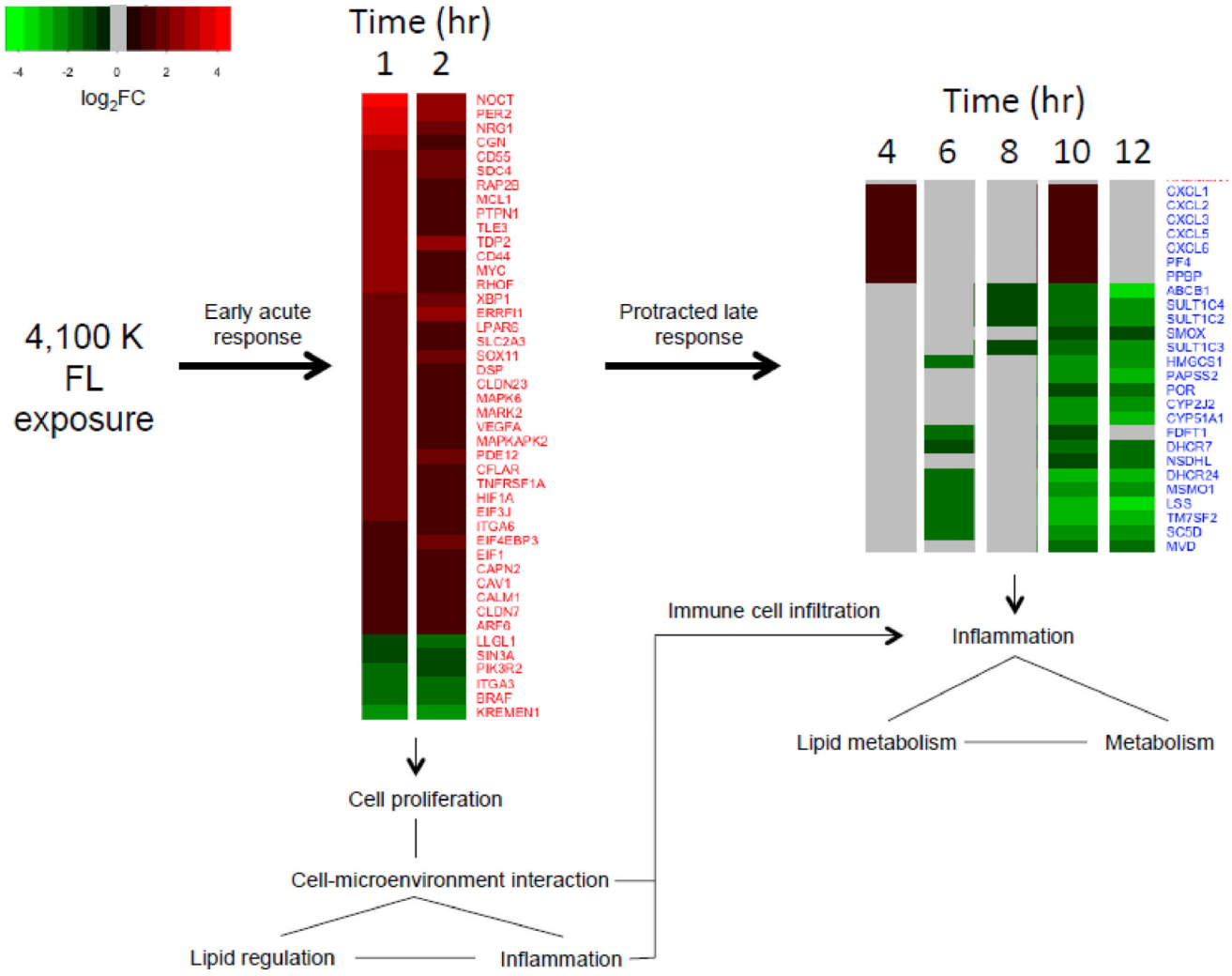

Figure 5. Differential expression of genes involved in the pathways representing the early and late genetic response

The pathways representing the early phase genetic response to FL (1 and 2 hr) involves 44 genes (red). Twenty-six genes are involved in pathways representing late phase genetic response (blue) to FL. After 1 to 2 hrs of FL exposure, cell-microenvironment interaction, as well as inflammation and lipid regulation related genes are predominantly activated while proliferation related genes are modulated in both directions. After 4 to 12 hrs following FL exposure, genes involved in inflammation remain transcriptionally activated, while genes involved with metabolism are repressed. The early phase gene expression response suggests the immune response (i.e., immune cell infiltration) is a result of functional changes in skin that may lead to the late phase gene expression response, involved with transcriptional activation of chemokines and suppression of lipid and small molecule metabolism. In the heatmap, green color represents down-regulated genes; red color represents up-regulated genes; gray color represents gene that didn't show differential expression.

Table 1

RNA-Seq Statistics

Time (hr)	Pre-Filtered Reads (M)	Filtered Reads (M)	Mapping Rate (%)	Transcriptome Coverage (X)
0(A)	58	43	89	24
0(B)	58	43	89	24
1(A)	58	43	89	25
1(B)	56	41	90	23
2(A)	58	42	90	24
2(B)	62	43	90	25
4(A)	50	37	89	21
4(B)	53	39	89	22
6(A)	50	36	89	21
6(B)	54	39	89	22
8(A)	59	44	89	25
8(B)	60	44	87	24
10(A)	60	44	89	25
10(B)	57	42	89	24
12(A)	59	42	90	24
12(B)	56	42	89	24

M = Million
% = Percent mapping
x= Fold Coverage

Table 2

Functional analyses of early phase and late phase genetic response

Early Response			
Function	**Canonical Pathways**	**−log(*p*-value)**	**Genes**
Cell-microenvironment Interaction	Tight Junction Signaling	1.70	CLDN23,TNFRSF1A,CGN,MARK2,CLDN7,LLGL1
Cell-microenvironment Interaction	Relaxin Signaling	1.35	VEGFA,PDE12,TDP2,PIK3R2,BRAF
Cell-microenvironment Interaction	Integrin Signaling	2.69	RAP2B,ARF6,ITGA6,CAV1,CAPN2,RHOF,BRAF,ITGA3,PI
Cell-microenvironment Interaction	Virus Entry via Endocytic Pathways	2.01	ITGA6,CAV1,PIK3R2,ITGA3, CD55
Cell-microenvironment Interaction	ILK Signaling	1.89	VEGFA,MYC,TNFRSF1A,HIF1A,RHOF,DSP,PIK3R2
Inflammation	Agranulocyte Adhesion and Diapedesis	1.47	CLDN23,TNFRSF1A,ITGA6,SDC4,CLDN7, ITGA3
Inflammation	eNOS Signaling	1.32	VEGFA,LPAR6,CAV1,PIK3R2, CALM1
Inflammation	Granulocyte Adhesion and Diapedesis	1.59	CLDN23,TNFRSF1A,ITGA6,SDC4,CLDN7, ITGA3
Inflammation	Regulation of eIF4 and p70S6K Signaling	1.30	EIF1,EIF4EBP3,EIF3J,PIK3R2,ITGA3,
Inflammation	IL-6 Signaling	1.63	VEGFA,TNFRSF1A,MAPKAPK2,MCL1,PIK3R2
Lipid regulation	Adipogenesis pathway	2.13	TNFRSF1A,XBP1,HIF1A,PER2,NOCT,SIN3A
Lipid regulation	Caveolar-mediated Endocytosis Signaling	2.68	PTPN1,ITGA6,CAV1,ITGA3, CD55
Proliferation	Wnt/b-catenin Signaling	1.67	MYC,MARK2,CD44,TLE3,SOX11,KREMEN1
Proliferation	HIF1_a Signaling	1.80	VEGFA,MAPK6,HIF1A,SLC2A3,PIK3R2
Proliferation	Ovarian Cancer Signaling	1.43	VEGFA,CD44,PIK3R2,SIN3A,BRAF
Proliferation	Neuregulin Signaling	2.27	NRG1,MYC,ERRFI1,PIK3R2,ITGA3
Proliferation	Molecular Mechanisms of Cancer	1.30	RAP2B,MYC,HIF1A,CFLAR,RHOF,SIN3A,BRAF,ITGA3,PI
Late Response			
Function	**Canonical Pathways**	**−log(*p*-value)**	**Genes**
Inflammation	Agranulocyte Adhesion and Diapedesis	4.62	CXCL3,PPBP,PF4,CXCL1,CXCL5,CXCL2,CXCL6
Inflammation	Granulocyte Adhesion and Diapedesis	4.80	CXCL3,PPBP,PF4,CXCL1,CXCL5,CXCL2,CXCL6
Metabolism	Xenobiotic Metabolism Signaling	2.01	ABCB1,SULT1C4,SULT1C2,SMOX,SULT1C3
Metabolism	LPS/IL-1 Mediated Inhibition of RXR Function	4.17	ABCB1,SULT1C4,SULT1C2,SMOX,SULT1C3,HMGCS1,PA
Metabolism	Melatonin Degradation I	6.44	POR,SULT1C4,SULT1C2,CYP2J2,SULT1C3,CYP51A1
Metabolism	Superpathway of Melatonin Degradation	7.67	POR,SULT1C4,SULT1C2,SMOX,CYP2J2,SULT1C3,CYP5
Lipid metabolism	Cholesterol Biosynthesis I	18.4	FDFT1,DHCR7,NSDHL,DHCR24,MSMO1,LSS,TM7SF2,SC5D,
Lipid metabolism	Cholesterol Biosynthesis II (via 24,25-dihydrolanosterol)	18.4	FDFT1,DHCR7,NSDHL,DHCR24,MSMO1,LSS,TM7SF2,SC5D,
Lipid metabolism	Cholesterol Biosynthesis III (via Desmosterol)	18.4	FDFT1,DHCR7,NSDHL,DHCR24,MSMO1,LSS,TM7SF2,SC5D,
Lipid metabolism	Superpathway of Cholesterol Biosynthesis	18.7	MVD,FDFT1,DHCR7,NSDHL,DHCR24,MSMO1,LSS,TM7SF2,HMGCS